KSCE Journal of Civil Engineering (2018) 22(1):174-184
DOI 10.1007/s12205-017-0636-4

Structural Engineering
pISSN 1226-7988, eISSN 1976-3808
www.springer.com/12205

High-Strength Model Material Production for Structural Plane Replica and Its Shear Testing

Feng Ji*, Changjiang Liu, Yu Zhang***, Luobing Zheng****, Kai Pan*****, and Xun Tan********

Received October 27, 2015/Revised 1st: August 20, 2016, 2nd: December 12, 2016/Accepted Janaury 19, 2017/Published Online April 6, 2017

Abstract

Shear strength parameters (c, φ) of a structural plane are the key factors for the stability assessment of rock masses. The shear strength parameters are obtained by a structure plane shear test carried out in laboratory. However, it is difficult to obtain test samples with the same surface morphology and to remove the effect of surface irregularity from test results. Based on the similarity principle and orthogonal test, this paper presents a new model preparation method for structural planes using a high-strength mold mixture material. Firstly, the original morphology of the structural plane is recorded by in situ measurement using a laser device and then the mold of the structural plane is reproduced using a 3D printer. Subsequently, a mix proportion test of the high-strength mold material is conducted using the orthogonal test, and the model of the structural plane is prepared by pouring this high-strength mixture material into the 3D mold. Ultimately, the shear strength parameters of this high-strength structural plane replica are obtained using a shear box test in the laboratory. The proposed method has particular advantages such as the preparation of multiple replicas for structure planes and the ability to obtain repeatable results.

Keywords: *structural plane, physical simulation, high-strength mold material, mix proportion, laser scanner, 3D print, shear test*

1. Introduction

Structural planes clearly affect the stability of rock masses (Barton and Choubey, 1977). Currently, laboratory shear tests are very common methods for obtaining the strength parameters of a structural plane (Fig. 1). However, the roughness of structural plane surfaces varies from one point to another. Different sections of structural plane surfaces are quite likely to yield significantly different results from shear tests, severely affecting the accuracy of projects. It is also well known that the shear strength parameters of a structural plane are mainly related to three factors: the Joint Compressive Strength (JCS), the Joint Roughness Coefficient (JRC), and the joint basic friction angle (Barton and Choubey, 1977). With the rapid development of measuring instruments and relevant experimental materials, empirical modeling work of a structural plane has become feasible. However, there is no specialized research on structure planes' multiple replicas and its shear testing that integrates these new materials and new methods. All of the available research has been performed independently, and the results have not been integrated for a modeling experiment that includes joint parameters.

Model tests are widely used in literature for solving complex engineering problems. A physical model of a structural plane was introduced decades ago to study the slope angle effect of serrated structures on gypsum (Patton, 1966). Morphological effects of the structural surface were later explored in a mechanical model using gypsum powder (Chou, 1979). The cut mechanism of serrated structure planes was simulated using a plaster model (Einstein, 1983). Later, several scholars made different physical models for research on different problems. Table 1 provides information regarding these materials and methods used for producing structural plane models for shear testing.

Mixed materials obtained by mixing iron ore powder, barites

*Associate Professor, State Key Laboratory of Geohazard Prevention and Geoenvironment Protection, Chengdu University of Technology, Chengdu 610059, China (E-mail: 65341207@qq.com)
**Associate Professor, State Key Laboratory of Geohazard Prevention and Geoenvironment Protection, Chengdu University of Technology, Chengdu 610059, China (Corresponding Author, E-mail: changjiangliucd@126.com)
***Ph.D. Student, State Key Laboratory of Geohazard Prevention and Geoenvironment Protection, Chengdu University of Technology, Chengdu 610059, China (E-mail: zhang_y3@cdut.edu.cn)
****Ph.D. Student, State Key Laboratory of Geohazard Prevention and Geoenvironment Protection, Chengdu University of Technology, Chengdu 610059, China (E-mail: zheng_lb@cdut.edu.cn)
*****Ph.D. Student, State Key Laboratory of Geohazard Prevention and Geoenvironment Protection, Chengdu University of Technology, Chengdu 610059, China (E-mail: pankai2@cdut.edu.cn)
******Ph.D. Student, State Key Laboratory of Geohazard Prevention and Geoenvironment Protection, Chengdu University of Technology, Chengdu 610059, China (E-mail: Tan_x3@cdut.edu.cn)

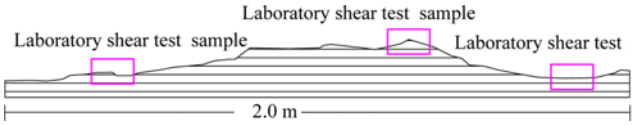

Fig. 1. Profile Morphology of the Structural Plane. This Shows that when the Laboratory Shear Test Samples are Selected from Different Parts of the Same Structure, Since the Structure Surface Morphology Varies, it Leads to Unreliable Experimental Results

powder, sand, rosin, and gypsum powder with alcohol, have advantages such as high density, stable performance, easy dryness, and excellent flexibility (Wang *et al.*, 2006). Su *et al.* (2008) studied the influence of samples consisting of aggregate and cement. Yang *et al*. (2000) tested the serrated rough surface of a rigid structural plane model using plaster, and explicitly considered the shear direction angles in which surfaces were arranged for angles of 30° and 15°. Kwon *et al.* (2010) studied the effects of different ratio (H/L_A) values on the shear results by using gypsum as the material, setting up controlling parameters in the height (H), length (L_A), and ratio (H/L_A) of rectangular convex bodies. Morelli (2014) described the fluctuation of a ladder type structure. Babanouri (2014) studied the shear behavior of the rectangular structure model by controlling the height and the length, using gypsum as a raw material. Zhao and Peng (2011) simulated soft rock with sand and a binder, and the results showed that the physical and mechanical properties of the materials for the chosen ratios, such as uniaxial compressive strength tests, elasticity modulus, tensile strength, internal frictional angle, and Poisson's ratio, correlated well with the mechanical properties of soft rock. Zhang *et al.* (2009) analyzed physical parameters with a mixture of rubber powder and water cement, and a new material similar to rock was produced. Du *et al.* (2010) mixed high-strength cement, silica fume, super plasticizer, and standard sand with water, which was able to be used to cover low and medium-intensive rock by adjusting the content of different materials. Huang *et al.* (2013) obtained joint plane morphology by pouring concrete into the joint plane. In addition, many scholars have made a regular rough surface mold using a Polyvinyl Chloride (PVC) plate (Du *et al.,* 2010; Huang *et al*., 2013a, b; Luo *et al.*, 2014). Luo *et al.* (2014) prepared model material by mixing sand, cement, silica powder, and a naphthalene super plasticizer of non-air entraining, and obtained a model material that is quite similar to natural calcareous slate in terms of the physical and mechanical properties.

On surface topography roughness evaluation, Turk *et al.* (1987) adopted a fractal theory for the characterization of irregular joint surface profiles, which showed that rock joint surface roughness can be represented by a fractional number called a fractal dimension (D). The self-similarity concept of fractals suggests that as the measuring step length (E) decreases, the total joint profile length (L) increases, as shown by the fundamental relation: Log (L) = (l-D) Log (E). Feng *et al.* (2003) proposed a new method for in situ non-contact measurements of the fracture roughness by using a Total Station (TS). Morelli *et al.* (2014) put forward a new concept to describe the degree of roughness of joints.

Gypsum is widely used in model making as it has easy model forming characteristics, and can be obtained easily and handled conveniently. However, cement does not have the best effect when it reaches its final set strength (Huang *et al.*, 2013b).

As mentioned previously, most literature for structure surface morphology shear testing uses regular-shaped asperities, and production methods of the irregular surface of rock joints is relatively infrequent in literature (Huang *et al.*, 2013a, b). In addition, for most materials that are used to simulate rock, the

Table 1. Materials and Properties Used for Laboratory Shear Testing

Researcher	Material and mix proportion by weight	Mechanical parameters of materials		Shape of the asperities
Patton (1966)	Gypsum:ground quartz sand: water = 3:1:1.48	Residual friction angle φ_r	34~36°	Sawtooth, rectangle
		Compressive strength	1.02 MPa	
	Gypsum: kaolinite:water = 1:1:0.96	Residual friction angle φ_r	27~28°	
		Compressive strength	0.66 MPa	
Chou Ruiguang, Chen Shicai, Sun Guangzhong (1979)	Gypsum	Uniaxial compressive strength	4.12 MPa	Sawtooth
		Cohesion c	0.59 MPa	
		Internal friction angle φ	45°	
Changyi (2000) Yang *et al*. (2000)	Gesso:water = 1:0.6	Uniaxial compressive strength	7.36 MPa	Sawtooth
		Basic friction angle φ	35°	
Wang *et al.* (2006) Sue *et al.* (2008) Kwon *et al*. (2010)	Gypsum:water = 3:2	Cohesion c	2.5 MPa	Rectangle
		Internal friction angle φ	41°	
		Residual friction angle φ	40°	
		Basic friction angle φ_b	39°	
Du *et al*. (2010)	Sand:water:water reducer:silicon powder: cement = 1.5:0.3:0.0015:0.1:1	Compressive strength	78.1 MPa	-
		Unit weight	23.03 kN/m^3	

compressive strength is not more than 30 MPa (Table 1). Moreover, during the modeling process, it is difficult to pour and reproduce an original joint morphology by covering a thin film on a joint plane and pouring mortar on such a thin film. Therefore, it is practically significant to find a new method to produce a mold having the same shape of rough structural surfaces.

In this paper, a new method is proposed called the physically modeled structural plane shear testing method. Its purpose is to measure the failure mechanism of structural planes. Firstly, the structural plane's morphology was recorded using a laser scanner, and its surface appearance was established by a 3D printer. Subsequently, test samples, which were similar to the original structural plane by having similar morphology and asperity angle and heights, were produced by using developed high-strength materials. Ultimately, the shear strength parameters of the structural plane were found by performing shear box tests, in which dilation angles were measured. This proposed method has several advantages, including that multiple representative test samples of identical structural plane surfaces can be prepared in laboratories, and their results are reproducible.

2. Materials and Methods

A mix proportion procedure was obtained for preparing high-strength model material for a structural plane, with the ratio between cement and sand as 1:1.5; the ratio between cement and water as 1:0.3; and the ratio between sand and gravel as 4:1. In addition, 1.5% water reducer, 2% accelerator, 10% silicon powder, and 15% silicon carbide, each of the total mix, were used.

In order to select similar materials and carry out a mixture ratio test, geometrical characteristics and physical parameters of the material model must be in accord with the similarity principle. New high-strength model materials were developed by mixing 52.5R compound silicate cement, fine sand, coarse sand, gravel of 3-6 mm, green silicon carbide (SiC), and micro silicon powder. The 52.5R compound silicate cement contained glue, with fine sand and grit as fine aggregates, gravel of 3-6 mm as a coarse aggregate, green SiC, and an early-strength admixture, with micro silicon powder used as additive. In order to find the best mix proportions of the test materials, multi-parameter orthogonal tests were conducted. All the used raw materials are shown in Fig. 2. Moreover, cube samples were prepared to direct shear test for their compressive ,shear and tensile strengths. The dimensions and testing standards of the modulus materials are given in Table 2.

The procedure given in the flow chart (Fig. 3) was followed for the development of the high-strength material and the shear testing of the structural plane models.

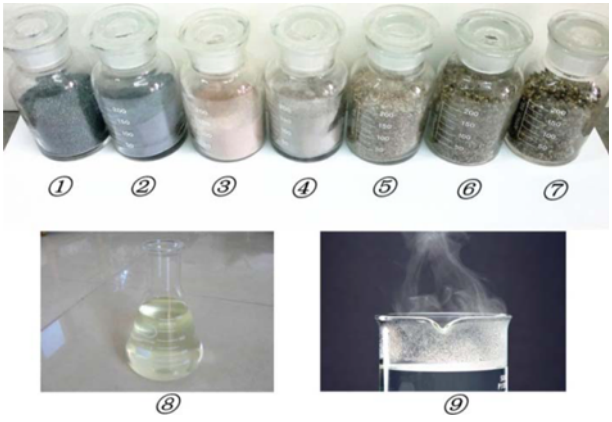

Fig. 2. Components of Similar Raw Materials: ① Green SiC, ② Micro Silicon Powder, ③ Early-strength Admixture, ④ Portland Cement, ⑤ Fine Sand, ⑥ Coarse Sand, ⑦ Aggregate (3-6 mm), ⑧ Carboxylic Water-reducer, ⑨ Warm Water (30-45°C)

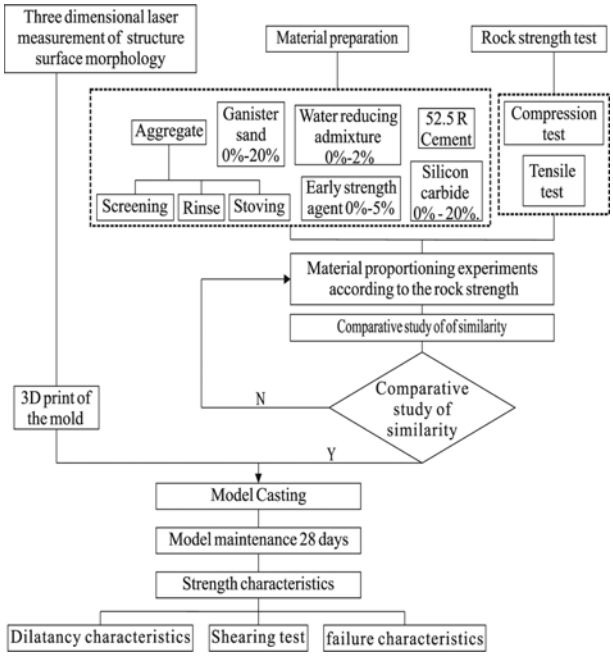

Fig. 3. Model Preparation Procedure of the Structure Plane Replica

3. Results and Analysis of Material Combination and Model Design

3.1 Orthogonal Test of Fineness Modulus and Cement Sand Ratio

Fineness modulus of the tested materials were performed, and

Table 2. Testing Type, Specimen Dimensions and Standard Use in Testing

Testing type	specimen dimensions	standard
Comprehensive strength	ϕ50 × 100 mm	ASTM (American Society for Testing Material) ISRM (International Society for Rock Mechanics)
Tensile strength	ϕ50 × 50 mm	
Shear strength	100 × 100 × 100 mm	

Table 3. Comprehensive Strength (MPa) of Material Fineness Modulus and Cement–sand Ratio

Fineness modulus	Cement–sand ratio							
	1:1	1:1.2	1:1.4	1:1.5	1:1.6	1:1.7	1:1.8	1:2.0
1.8	50.12	56.21	60.51	66.55	64.29	60.56	58.33	57.14
2	51.02	59.13	63.45	68.23	65.14	63.78	62.01	58.02
2.2	52.13	60.23	68.47	74.3	70.61	68.14	63.55	57.31
2.4	52.35	63.45	70.58	78.42	73.21	70.21	64.48	60.45
2.6	53.37	64.28	75.26	80.21	75.42	70.89	67.38	64.11
2.8	57.85	65.18	78.64	***84.33***	78.23	72.87	68.16	66.14
3	56.34	63.88	72.38	78.22	74.35	71.25	67.65	65.17
3.2	51.27	59.21	69.17	74.27	71.59	69.71	65.48	61.22

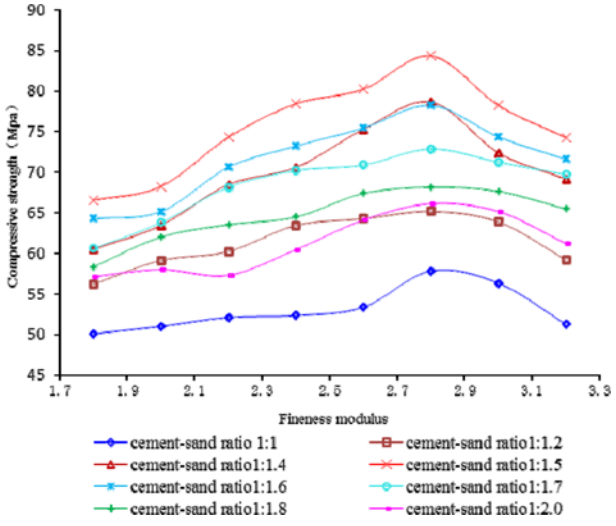

Fig. 4. Compressive Strength Versus Material Fineness Modulus for Different Cement–sand Ratios

the results are shown in Table 3. The cement-sand ratio shows that the material strength went up with an increased amount of cement, but dropped when the total amount of cement reached a threshold value of a cement-sand ratio of 1:2.8 (Fig. 4). It was also found that the mortar strength was the highest when the fineness modulus of the sand was between 2.5 and 3.0. Through a series of material proportion tests and comprehensive strength tests, it was established that the best cement–sand ratio was 1:1.5, and the best fineness modulus was 2.804. The experimental data and strength parameter curves are shown in Table 2 and Fig. 4, respectively.

3.2 Effects of Material Curing Time

Tests for tensile, compressive, and shear strength were carried out on the prepared mold material using ISRM standard. The strength curve of the model material strength (tensile, compressive, and shear) with curing time is given in Table 4, and their plots are shown in Fig. 5.

The strength of the samples cured for 7 days and 28 days were compared, and the tensile, compressive, and shear strengths were found to increase by 2.28%, 5.67%, and 5.35%, respectively, with increased cure time (Table 3).

Table 4. Variation of the Material Strength with Curing Time

Curing time (day)	Tensile strength (MPa)	Compressive strength (MPa)	Shear strength (MPa)
4	4.03	37.53	4.69
7	6.26	58.29	7.28
14	6.38	59.41	7.42
28	7.09	66.02	8.25

time（day）	strength(MPa）	strength （MPa）	（MPa）
4	4.03	37.53	4.69
7	6.26	58.29	7.28
14	6.38	59.41	7.42
28	7.09	66.02	8.25

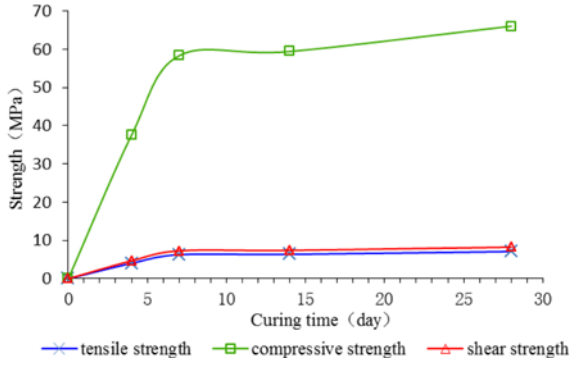

Fig. 5. Model Material Strength Variation With Curing Time

3.3 Mixture Ratio Test of Water Reducer

The function of a water reducer in mortar is to lubricate, disperse, and to cause steric hindrance (Huang *et al.*, 2013a) of the model materials. A polycarboxylate super plasticizer, which is a viscous liquid of light yellow color, was added at a maximum amount of 1.5% of the total mixture. From Fig. 6, it is clear that the compressive strength of the samples increased rapidly when the amount of admixture was increased from 0% to 1.5%, but the rate of such increases slowed when the total amount of added admixture was over 1.5%. In order to study the effect of the water reducer, further tests (tensile, compressive, and shear) were carried out using water reducer of the amount of 1.5% of the total amount of the mixture. As observed from the

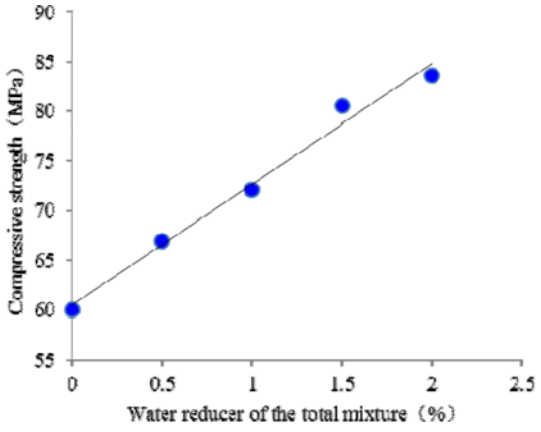

Fig. 6. Relationship between the Amount of Water Reducer and Compressive Strength

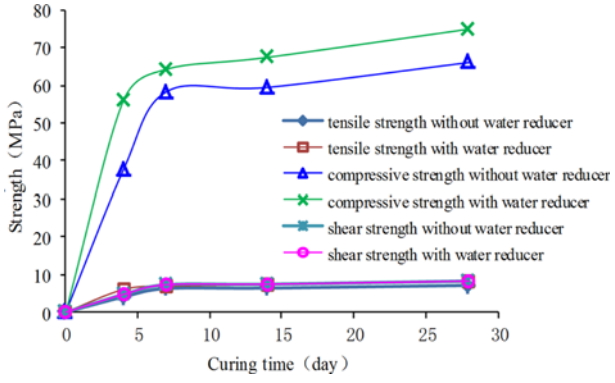

Fig. 7. Strengths Variation with Water Reducer of 1.5% of the Total Mix

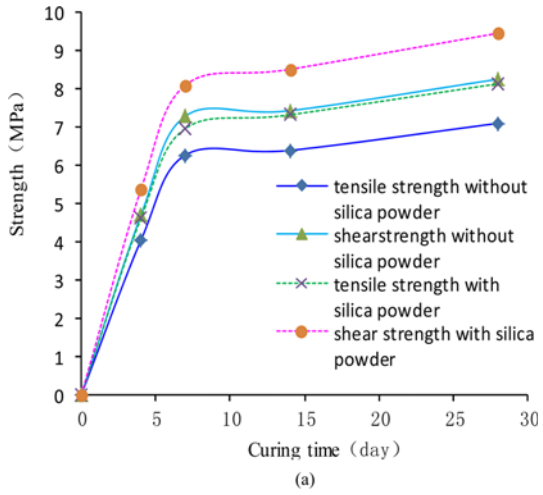

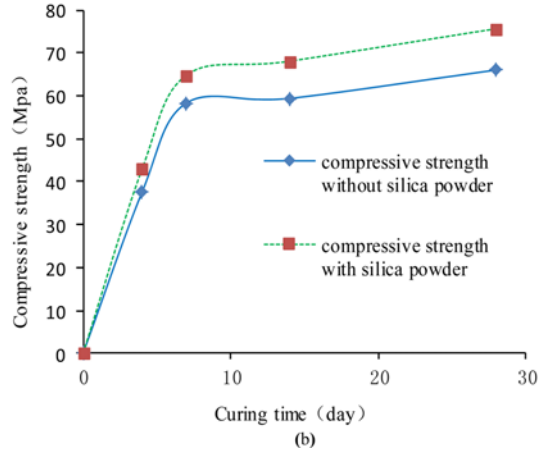

Fig. 8. Strength Characteristics after Adding Silicon Powder for the Model Mix: (a) Plot of the Tensile and Shear Strengths Against the Curing Time, (b) Plot of the Compressive Strength against the Curing Time

test results shown in Fig. 7, the compressive strength increased from 6 to18 MPa after the addition of the water reducer

3.4 Mixture Ratio Test of Silicon Powder

Silicon powder is an industrial dust generated by the reduction reaction of high purity quartz with coke during the process of smelting silicon under high temperature (>2000ºC). Significant improvement in the strength of the mold material is obtained when it was mixed with model material (Du *et al.*, 2010).

Experimental research has showed that when the dosage of silicon powder is more than 20% of the total gelled material, its efficiency declines significantly (Du *et al*., 2010). However, when the dosage is over 30%, the material strength decreases, cracking and shrinkage risk of the model material increases, construction difficulties occur, and costs are expected to increase. In the field of practical engineering, the dosage is controlled between 5% and 15% (Huang *et al*., 2013a). For this research, the dosage of silicon powder used was 10% when the contrast test was conducted. The changes in the tensile, shear, and compressive strengths after the addition of silicon powder are shown in Figs. 8(a), (b). It can be observed that the strength of cement mortars increased by 10-20% when silicon powder was added.

3.5 Mixture Ratio Test of Silicon Carbide

Studies regarding the use of Silicon Carbide (SiC) are scarce in literature. SiC can enhance the performance of a material when it is mixed with concrete mortar (Du *et al.*, 2010). For this study, a comparative trial on cement mortar adding silicon carbide at 0%, 5%, 10%, 15% and 20% ratios was conducted. The relationship between the tensile and comprehensive strength and curing time and dosage is shown in Figs. 9(a), (b).

According to the experiments shown in Fig. 9(a), (b), SiC significantly improved the strength of the model material. When the dosage was more than 20%, the range of the strength increase was not clear. Therefore, the ideal dosage is between 15% and 20% (Figs. 9(a), (b)). In this experiment, a dosage of 15% SiC was used, giving a compressive strength of 82.77 MPa, which was 16.75 MPa higher than the mortar SiC, at the growth rate of 25.4% (Fig. 9(b)). Furthermore, a dosage of 20% showed a shear strength of 10.034 MPa, which was 2.09 MPa higher than the mortar without SiC, at the growth rate of 25.4% (Figs. 9(c)).

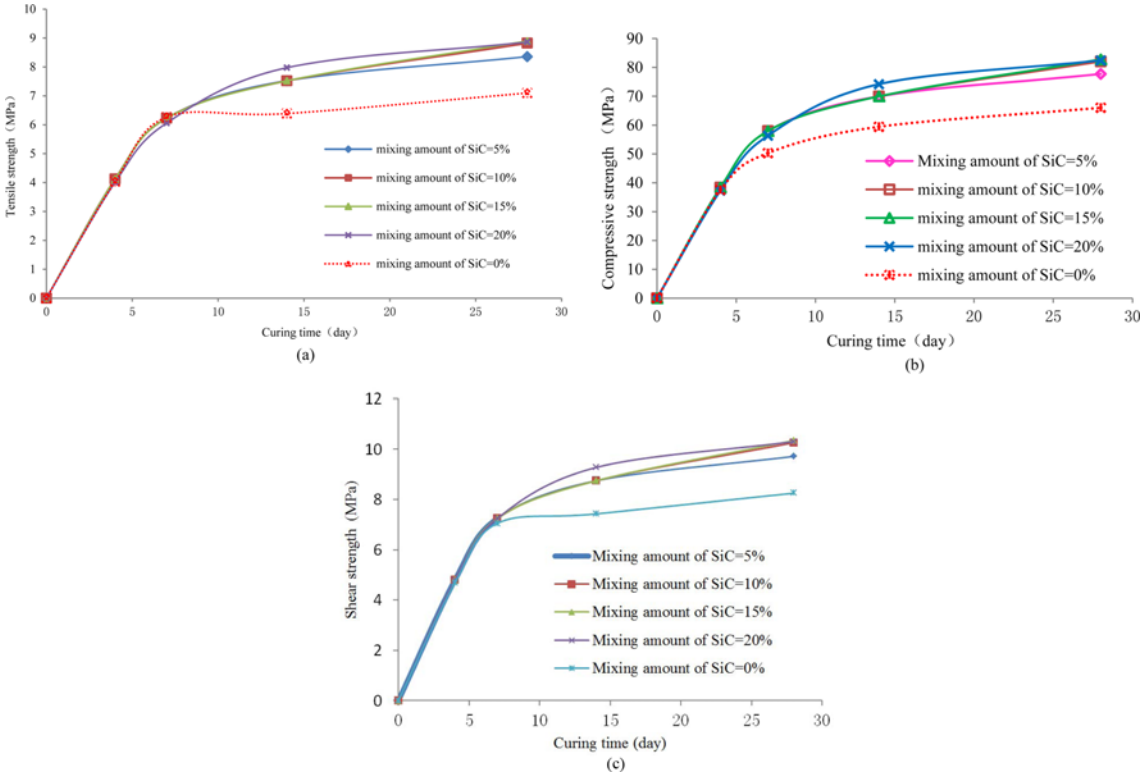

Fig. 9. The Relationship Between the Model Material Strengths and the SiC Ratios: (a) Relationship between Tensile Strength and SiC Ratio of the Modal Material, (b) Relationship between the Compressive Strength and the SiC Ratio of the Model Materials, (c) Relationship between the Shear Strength and the SiC Ratio of the Model Materials

Through the aforementioned mixture ratio test, it was possible to obtain a mix proportion procedure for the preparation of high-strength model materials to produce shapes of structural planes. The optimum ratio of the strong mixture ratios was found to be at 1:1.5 between cement and sand, 1:0.3 between cement and water, and 4:1 between sand and gravel. In addition, optimum amounts ratios were found to be 1.5% for the water reducer, 2% for the accelerator, 10% for the silicon powder, and 15% for silicon carbide.

The new simulation material has a wide range of adjustable strength by changing the admixture ratio of the mixture samples. With the appropriate adjustment of the dosage of raw materials, simulated materials with different strengths can be obtained which can meet requirements of model shear tests of a structural plane.

3.6 Two-dimensional Surface Measurement, 3D Print and Modeling

The three-dimensional surface of a structural plane is the key factor that influences the shearing motion of a sample and its strength parameters. A 3D laser scanner (ZS Scanner 800) and 3D printer (UPrint SE Printers made by Stratasys) were used to measure the structural plane's morphology (Fig. 3). Following that, the structural plane appearance was printed using a three-dimensional printer. The technical processes for the structural surface model production are given below:

(1) First, the representative model is placed at the bottom, and the mold release agent is applied on the surface of the bottom mold. Then the outline box is installed.

(2) The surface model is prepared by pouring the mixture into the model box. The mixing materials are stirred and vibrated slowly using a vibrating tube.

(3) After pouring, the model material in the outline box model of the structural plane should be cooled for at least 24 h in the air at 20°C, followed by standard curing for 28 days under normal atmospheric conditions.

By using three-dimensional laser scanning and three-dimensional printing technology, the recorded accuracy of the sample surface can reach up to 0.1 mm. Therefore, this proposed method of production of the joint morphology, and the modeling precision of the three-dimensional irregular structure model, surpasses the traditional method, which can only produce a regular structural surface.

4. Shearing Test and Discussion

4.1 Joint Roughness Characterization and its Quantitative Description

The sample morphology of the structural plane is shown in Fig. 10. Red paint was applied to the surface of the structure so as to clearly observe the damage area and its extent during the shear testing.

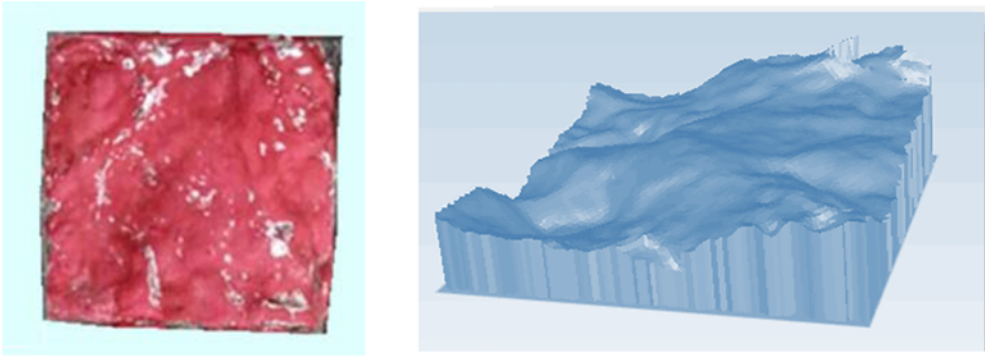

(a) (b)

Fig. 10. Morphology of a Structural Plane: (a) Shear Test Sample, (b) Vector Diagram of Structural Plane

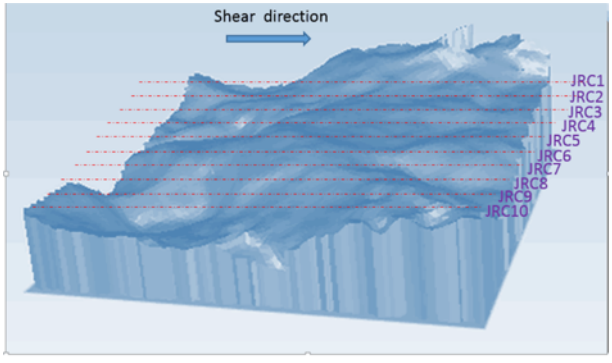

(a)

Serial number	Curve morphology
1	
2	
3	
4	
5	
6	
7	
8	
9	
10	

(b)

Fig. 11. Mesh Generation and Curve Morphology of Structural Plane: (a) Mesh Generation of Structure Morphology, (b) Structural Morphology of Different Parts

In the direction parallel to the shear, the surface structure was divided into 10 portions. The surface topography was measured at every 1 cm (Fig. 11), and the cure morphology of the profiles obtained before and after the shear testing are shown in Table 5.

4.2 Dilation Angle Evolution During the Shear Testing

Shearing experiments were carried out on the structural plane, and the resultant two-dimensional morphology of the sheared

Fig. 12. Morphology of Structure Surface after Shear Test

surface profiles are given in Table 5 of the sections given in Fig. 12.

The following conclusions were reached after the shear testing of the model structural planes:

(1) During the shearing, the damage occurred more seriously in the front of the specimens, and the damage was not apparent at the back of the specimens. This clearly shows that damage and climbing occur predominantly in the front end.

(2) At the locations where the asperity height was relatively large, the destruction of the asperity was more serious. However, in the low-lying parts, the damage was not apparent. This shows that during the shearing process, the stress distribution in every part is not uniform.

(3) In the shearing process, the profile asperity average height of the structural plane was reduced by 8.8%, the maximum height was reduced by 13.2%, and the reduction range varied in different positions of the section. Generally, the greater the profile asperity height of the original curve, the greater the magnitude of the reduction will be. The lower the profile asperity height of the original curve, the smaller the magnitude of the reduction will be. This suggests that the effect of the contribution of the anti-shear is more significant for structures with larger fluctuation degrees.

4.3 Shear Strength Characteristics

The direct shear tests were conducted on structural plane

Table 5. Dilation Angle Evolution During the Shear Testing (Hanging Side) of the Profiles Given in Table 5 of the Sections Given in Fig. 12

No.	Dilation angle evolution	Profile asperity average height / maximum height (cm)	
		Before the shear test	After the shear test
1	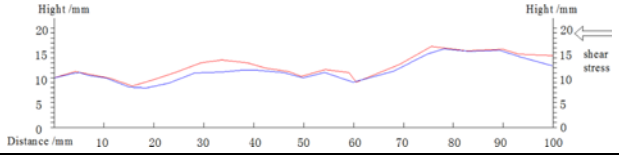	12.35 /16.3	11.55 /11.79
2	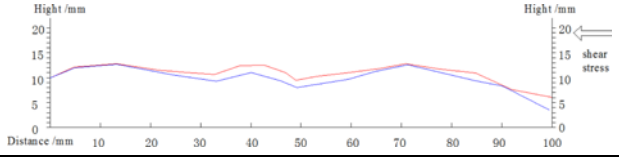	10.99 /12.74	10.07 /12.56
3	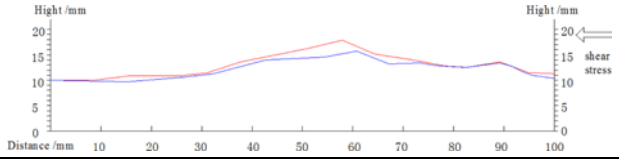	12.99 /17.88	12.28 /15.73
4	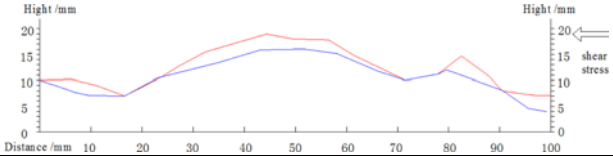	12.53 /18.95	10.99 /16.08
5	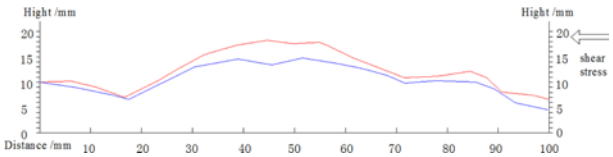	12.41/18.23	10.66/14.72
6	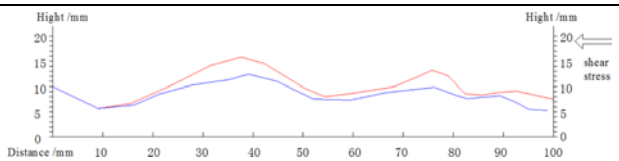	10.07 /15.79	8.52 /12.36
7	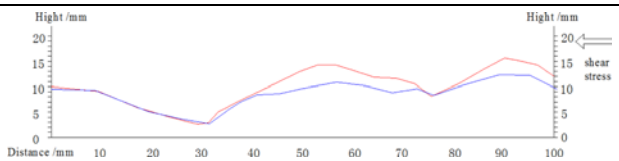	9.93/15.59	8.60/12.35
8	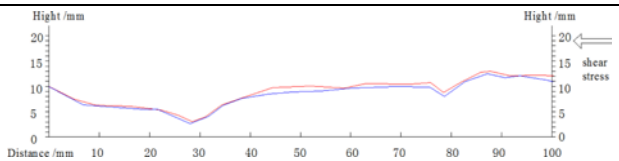	8.85 /13.00	8.35 /12.50
9	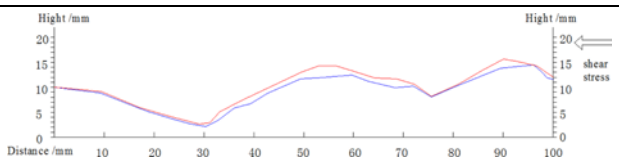	9.95 /15.6	9.15 /14.49
10	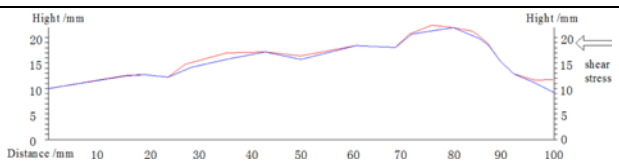	15.94 /22.44	15.55 /21.95
Average		11.6 /16.65	10.57 /14.45

Legend: Curve profile before shear test Curve profile after shear test

samples under different normal stresses (σ = 0.15, 0.3, 0.45, 0.6, 0.75 MPa) (Fig. 13), and their results are shown in Table 6. Due to good occlusion between the upper and lower structural plane surfaces, the shear break of the asperities was apparent, as shown in Fig. 13. According to a back calculation of the failure block under excavation, the parameter obtained from the shear test was close to the back calculation. Therefore, this proposed approach of carrying out the mechanical study of the structural plane using these model materials is feasible.

In addition, with an increase in the normal stress, the damaged section of the samples gradually increased (non-red paint region of Fig. 13). Under different stress conditions, the failure modes of the structural plane displayed different patterns. When the normal stress was between 0.15 MPa and 0.3 MPa, the trend line of the shear stress and the horizontal shear displacement was smooth, and the structure plane exhibited climbing movement. When the normal stress was between 0.45 MPa and 0.75 MPa, the trend line was steep, mainly due to the break of asperities after the climbing activity; in other words, when the normal stress was relatively low, the sliding failure was the main mode. As the normal stress gradually increased, the shear failure mode of the structural plane gradually changed from the sliding cutting damage type towards the sliding failure type. Relation curves of shear strength-shear strainş, vertical deformation-shear strain, and shear stress-normal stress were shown in Fig. 14.

Table 6. Shear Strength Parameters of the Model Structure Plane

Item	Parameters of shear test	Parameters of back calculation
φ(°)	44.09°	45°
C (MPa)	0.85 MPa	0.5 MPa

From the above data and the dilation effect, it was found that for the same strength material, the higher the normal stress level, the greater the failure area. The dilation effect is a combined result of the rock strength of structural plane, dilation angle, and normal stress. Moreover, there is a non-linear positive relationship between the loss area and the normal stress. Such a relationship has a logarithmic pattern, as shown in Fig. 15.

5. Conclusions

Based on the similarity principle and orthogonal test, a new model preparation method was presented for structural planes using high-strength mold mixture material. A laser scanner, 3D printer, shear tests, and dilation analysis were carried out in this study, the following conclusions were reached from the tests described previously.

1. High-strength model material was obtained using Portland cement of 52.5R grade as the binding material, medium-coarse and fine sand, gravel as the aggregate and water

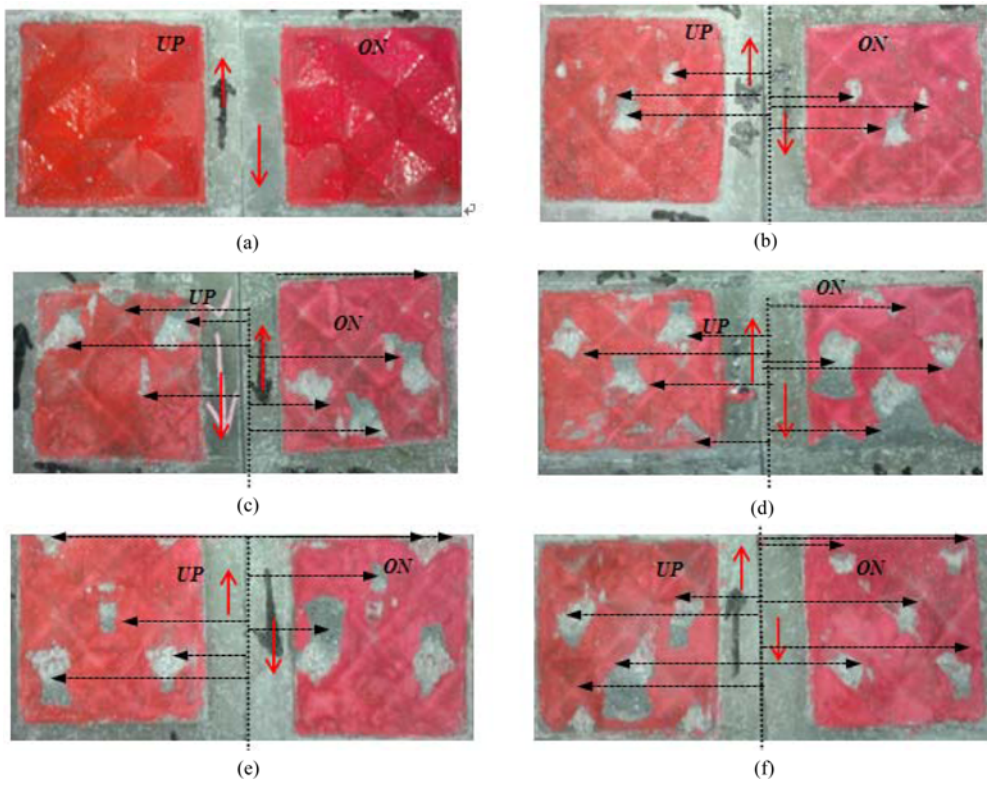

Fig. 13. Failure Type of Structural Plane under Different Normal Stress: (a) Structural Plane before Shear Test before Test, (b) Normal Stress (0.15 MPa), (c) Normal Stress (0.3 Mpa), (d) Normal Stress (0.45 MPa), (e) Normal Stress (0.60 MPa), (f) Normal Stress (0.75 MPa)

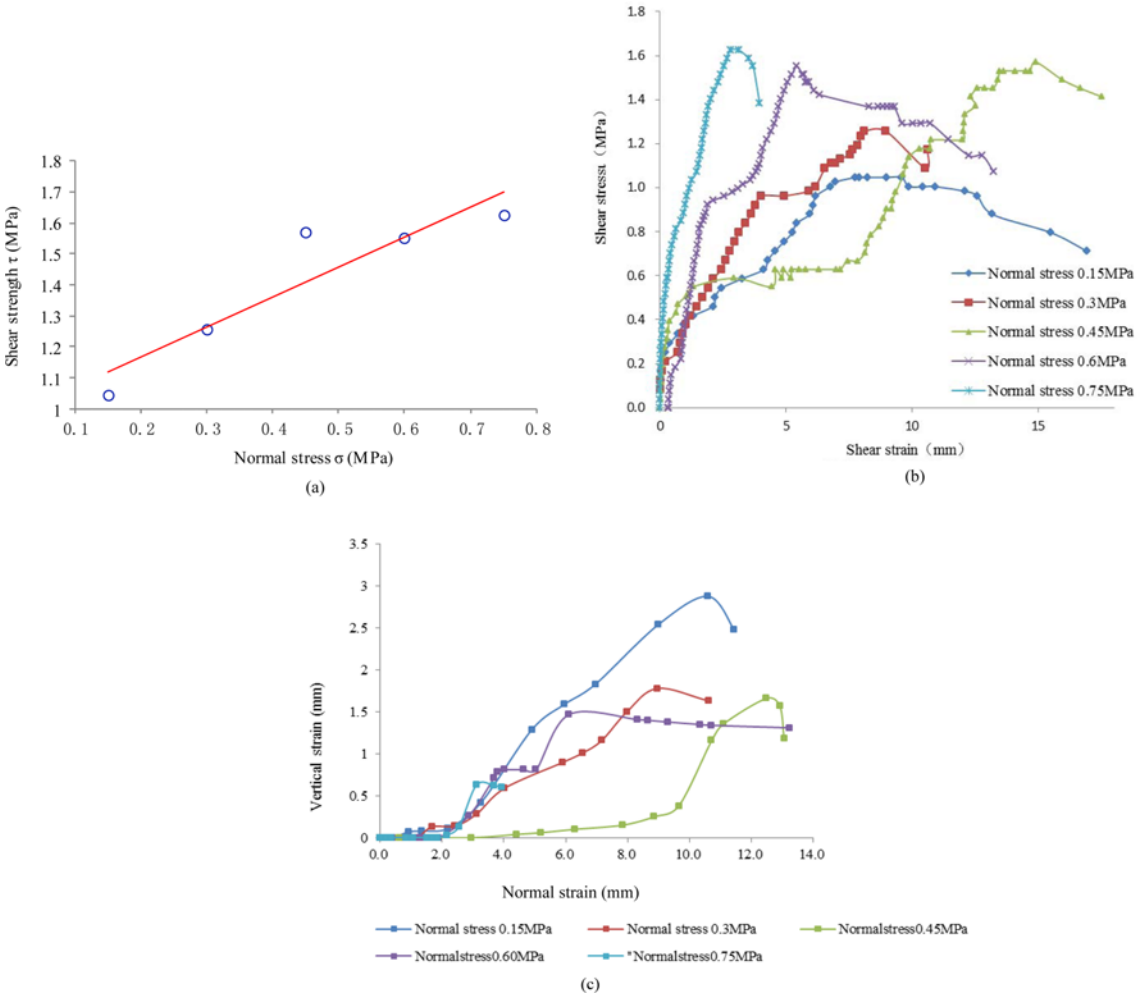

Fig. 14. Relation Curves of Shear Strength-shear Strain, Vertical Strain-shear Strain, and Shear Stress-normal Stress: (a) Relation Curves of Normal Stress and Shear Stress, (b) Relation Curves of Shear Stress and Shear Strain, (c) Relation Curves of Vertical strain and Shear Strain

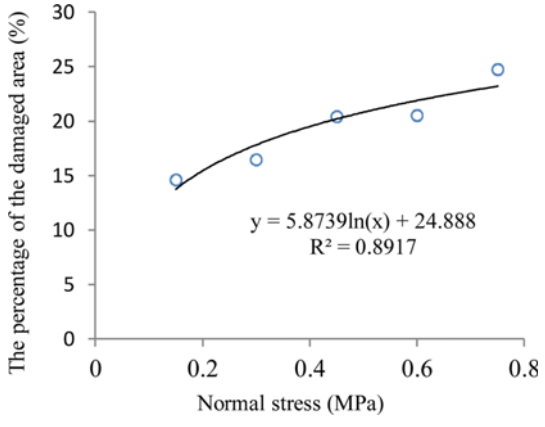

Fig. 15. Relationship between the Normal Stress and Percentage of the Damaged Area

reducer, and silicon powder with green SiC as additives. A mix proportion procedure was obtained for preparing high-strength model material for a structural plane, with the ratio between cement and sand as 1:1.5; the ratio between cement and water as 1:0.3; and the ratio between sand and gravel as 4:1. In addition, 1.5% water reducer, 2% accelerator, 10% silicon powder, and 15% silicon carbide, each of the total mix, were used.

2. A method of recording and producing a replica of the structural plane morphology using a Z S Scanner 500 and a U Prial SE Printer was developed.
3. For a two-dimensional irregular surface of the structural plane, the anti-shear contribution of the asperity body in the shear process was different. The result of the shear test is repeatable, and this method could provide reliable basic data for structural plane deformation and strength studies.

Acknowledgements

We acknowledge support by the National Natural Science Foundation of China (No. 51308082), the Key Fund Project of the Sichuan Provincial Department of Education (No. 15ZA0075), the Discovery Fund of the State Key Laboratory of Geohazard

Prevention and Geoenvironment Protection (SKLGP 00002296), the Talent Fund of Chengdu University of Technology (KYGG201303), and the China Postdoctoral Science Foundation (2013M540701). The authors are grateful to all of the technicians who worked in the laboratory of SKLGP for providing assistance throughout the experimental work, especially Dr. Dongpo Wang who provided advice on this research.

References

Babanouri, N. and Saeed Karimi Nasab (2014). "Modeling spatial structure of rock fracture surfaces before and after shear test: A method for estimating morphology of damaged zones." *Rock Mech Rock Eng.*, Vol. 32, No. 4, pp. 32-44, DOI: 10.1007/s00603-014-0622-9.

Barton, N. and Choubey, V. (0000). "The shear strength of rock joints in theory and practice[J]." *Rock Mechanics*, 1977, Vol. 10, No. 2, pp. 1-54.

Chou, R. G., Chen, S. C., and Sun, K. Z. (1979). "Experimental study on mechanical properties of serrate structure surface." *Geological Science*, No. 2, pp. 157-166.

Du, S. G., Huang, M., Luo, Z. Y., and Jia, R. D. (2010). "Similar materials study on mechanical prototype test of rock structural plane." *Chinese Journal of Rock Mechanics and Engineering*, Vol. 29, No. 11, pp. 2263-2270.

Einstein, H. H., Veneziano, D., and Baecher, G. B. (1983). "The effectof discontinuity persistence on rock slope stability." *International Journal of Rock Mechanics and Mining Sciences and Geomechanics*, Vol. 20, No. 5, pp. 227-236.

Feng, Q. H., Fardin, N., Jing, L., and Stephansson, O. (2003). "A new method for in situ non-contact roughness measurement of large rock fracture surfaces." *Rock Mechanics and Rock Engineering*, Vol. 36, No. 1, pp. 3-25, DOI: 10.1007/s00603-002-0033-1.

Huang, M., Du, S. G., Luo, Z. Y., and Ni, X. H. (2013). "Study of shear strength characteristics of simulation rock structural planes based on multi-size direct shear tests." *Rock and Soil Mechanics*, Vol. 34, No. 11, pp. 3180-3186.

Huang, M., Luo, Z. Y., Du, S. G., and Zhang, X. Y. (2013). "Study of inverse controlling technology for series scales similar surface model making of rock structural plane." *Rock and Soil Mechanics*, Vol. 34, No. 4, pp. 1211-1216. (Chinese)

Kim, S.-H. and Jeong, J.-H. (2003). "Use of surface free energy properties to predict moisture damage potential of asphalt concrete mixture in cyclic loading condition." *KSCE Journal of Civil Engineering*, Vol. 7, No. 4, pp. 381-387, DOI: 10.1007/s12205-015-0367-3.

Kwon, T. H., Hong, E. S., and Cho, G. C. (2010). "Shear behavior of rectangular-shaped asperities in rock joints." *KSCE Journal of Civil Engineering*, Vol. 14, No. 3, pp. 323-332, DOI: 10.1007/s12205-010-0323-1.

Kwon, T.-H., Hong, E.-S., and Cho, G.-C. (2010). "Shear behavior of rectangular-shaped asperities in rock joints." *KSCE Journal of Civil Engineering*, Vol. 14, No. 3, pp. 142-156, DOI: 10.1007/s12205-010-0323-1.

Luo, Z. Y., Du, S. G., and Huang, M. (2014). "Experimental study of stress effect on peak friction angle of rock structural plane." *Chinese Journal of Rock Mechanics and Engineering*, Vol. 33, No. 6, pp. 1142-1148.

Morelli, G. L. (2014). "On joint roughness: measurements and use in rock mass characterization." *Geotechnical and Geological Engineering*, Vol. 32, No. 2, pp. 345-362, DOI: 10.1007/s10706-013-9718-3.

Patton, F. D. (1966). "Multiple modes of shear failure in rock." *Proceedings of the 1st Congress of International Society of Rock Mechanics,* Lisbon., pp. 509-513.

Su, W., Leng, W. M., Lei, J. S., and Liu, C. J. (2008). "Test study of similar material in rock mass." *Soil Engineering and Foundation*, Vol. 22, No. 5, pp. 73-75.

Turk, N., Greig, M. J., Dearman, W. R., and Ami, F. F. (1987). "Characterization of rock joint surfaces by fractal dimension." *The 28th US Symposium on Rock Mechanic*, pp. 1223-1236.

Wang, H. P., Li, S. C., Zhang, Q.Y., Li, Y., and Guo, X. H. (2006). "Development of a new geomechanical similar material." *Chinese Journal of Rock Mechanics and Engineering,* Vol. 25, No. 9, pp. 1842-1847.

Yang, Z. Y. and Chiang, D. Y. (2000). "Experimental study on the progressive shear behavior of rock joints with tooth-shaped asperities." *International Journal of Rock Mechanics and Mining Sciences & Geomechanics Abstracts*, 2000, Vol. 37, No. 8, pp. 1247-1259, DOI: 10.1016/S1365-1609(00)00055-1.

Zhang, N., Li, S. C., Li, M. T., and Yang, L. (2009). "Development of a new rock similar material." *Journal of Shandong University (Engineering Science)*, Vol. 39, No. 4, pp. 149-154.

Zhao, Y. and Peng, H. Y. (2011). "Experimental study on similarity materials for soft rock of deep-buried tunnels." *Journal of Coal Science & Engineering*, Vol. 17, No. 2, pp. 124-127, D OI: 10.1007/s12404-011-0203-4.